Werk

Jahr: 1983
Kollektion: fid.geo
Signatur: 8 Z NAT 2148:52
Digitalisiert: Niedersächsische Staats- und Universitätsbibliothek Göttingen
Werk Id: PPN1015067948_0052
PURL: http://resolver.sub.uni-goettingen.de/purl?PPN1015067948_0052

LOG Id: LOG_0030
LOG Titel: FENNOLORA recordings at NORSAR
LOG Typ: article

Übergeordnetes Werk

Werk Id: PPN1015067948
PURL: http://resolver.sub.uni-goettingen.de/purl?PPN1015067948
OPAC: http://opac.sub.uni-goettingen.de/DB=1/PPN?PPN=1015067948

Contact

Niedersächsische Staats- und Universitätsbibliothek Göttingen
Georg-August-Universität Göttingen
Platz der Göttinger Sieben 1
37073 Göttingen
Germany
Email: gdz@sub.uni-goettingen.de

J Geophys (1983) 52:119–130

Journal of Geophysics

FENNOLORA Recordings at NORSAR*

R.F. Mereu[1], S. Mykkeltveit[2], and E.S. Husebye[2]
[1] University of Western Ontario, London, Ontario, Canada, N6A 587
[2] NTNF/NORSAR, Post Box 51, N-2007 Kjeller, Norway

Abstract. During August 1979 a number of major shots belonging to the FENNOLORA deep seismic sounding experiment across Scandinavia were recorded at NORSAR. The 42 sensors of the NORSAR array enabled us to examine both in-line and off-line features of the seismic signals as the wavefronts swept across the seven subarrays. A least squares analysis of the first arrival data indicate that the upper mantle velocities under NORSAR are azimuth dependent and vary from 8–9 km/s laterally. The data can also be used to infer approximate crustal thicknesses beneath shot points within 700 km.

A detailed analysis of the coda following the first arrival onsets was made using various velocity filters and correlation detectors to determine if any deterministic multiple arrivals arising from sharp large-scale regional vertical velocity gradients in the upper 300 km of the mantle were present. No later arrivals which were coherent beyond a few kilometers were found. We take this to indicate that scattering particularly in the source and receiver regions is of major importance in the generation of the seismic coda.

Key words: Deep seismic sounding – NORSAR array – FENNOLORA experiment – Crustal thickness – Crustal heterogeneity – Scandinavia – scattering

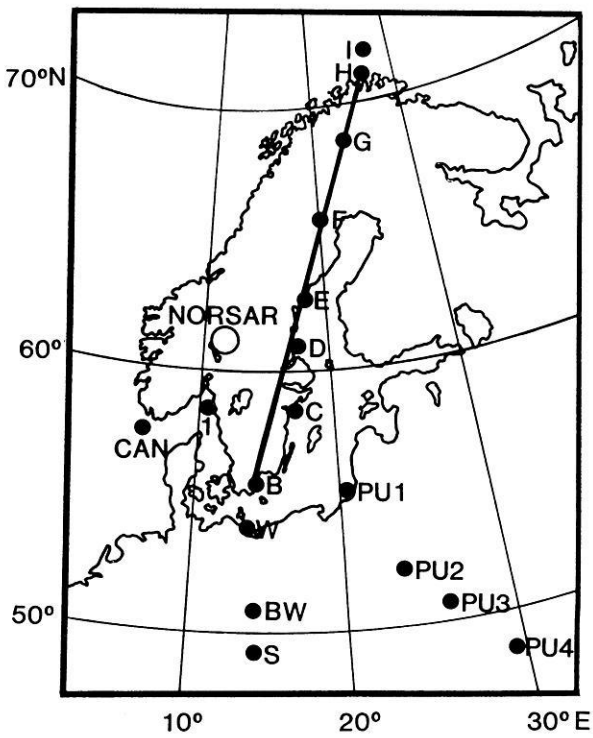

Fig. 1. Station and shot-point locations for the FENNOLORA long range experiment. Also shown is a shot-point belonging to the CANOBE experiment (CAN, Cassell et al., 1983), the location of a presumed explosion (1) in the sea about 260 km due south of NORSAR as well as the location of the NORSAR array

Introduction

During the month of August 1979 a major long-range seismic profile called the FENNOLORA experiment was carried out across Scandinavia. Charges ranging in size from 700–8,000 kg of TNT were fired at locations shown in Fig. 1, where also the main line deployment of mobile seismic stations is shown. Technical details of this experiment in terms of shot point information, etc., have been given by Ansorge (1981). In this paper the results obtained from analysis of recordings made at the NORSAR array are presented.

Most of the major shots (i.e., B, C, D, E, F, H, and I in Scandinavia, PU1 in Poland and PU3 in the USSR) were well recorded by the short-period sensors of NORSAR. Shots at G, W, BW, S, PU2 and PU4 were not detected. In order to improve the azimuthal coverage, the recordings from one of the CANOBE (CAN) shots of July 1980 (Cassell et al. in press, 1983) were also included in this study. Altogether the NORSAR records presented here cover the distance and azimuth ranges shown in Table 1. The configuration of the 7 subarrays and 42 short-period sensors making up the NORSAR array at the time of the FENNOLORA experiment is shown in Fig. 2.

In most seismic experiments where portable instruments are deployed, off-line coverage is not obtained. In this experiment the two-dimensional areal extent of the whole NORSAR array has enabled us to examine both the in-line and off-line features of the seismic signals as the wavefronts

* NORSAR Contribution No. 322

Offprint requests to: R.F. Mereu

Table 1. Shot point data and apparent velocities

Shot	Distance range (km)	Azimuth[a] range (km)	Apparent *Pg* velocity (km/s)	Apparent *Pn* velocity (km/s)
D2	315– 375	87– 97	6.53±0.64	8.65±0.13
E1	360– 420	63– 69	6.28±0.38	8.50±0.37
C1	415– 485	122–130	7.31±0.28	8.06±0.27
CAN	453– 515	219–225	6.63±0.22	8.08±0.14
B3	585– 665	149–155	6.28–0.14	8.38±0.24
F1	630– 695	34– 41		8.18±0.31
PU11	895– 972	136–141		8.38±0.20
H1	1,335–1,396	20– 22		8.14±0.19
I1	1,335–1,396	20– 22		8.99±0.99
Complete set	315–1,396	20–225	6.36±0.02	8.31±0.01

[a] The azimuth values are from NORSAR to the sources

Table 2. Delay times and crustal thicknesses

Shot	Distance to array center x(km)	Travel time to array center t(s)	Delay time (s) $t-x/8.1$	Azimuth (degrees)
CAN	456.7	62.5	6.1	220.0
B3	616.2	83.1	7.0	150.0
C1	451.5	64.3	8.6	123.0
D2	364.0	53.3	8.4	87.6
E1	414.3	60.1	9.0	62.3
F1	690.8	94.3	9.0	37.0

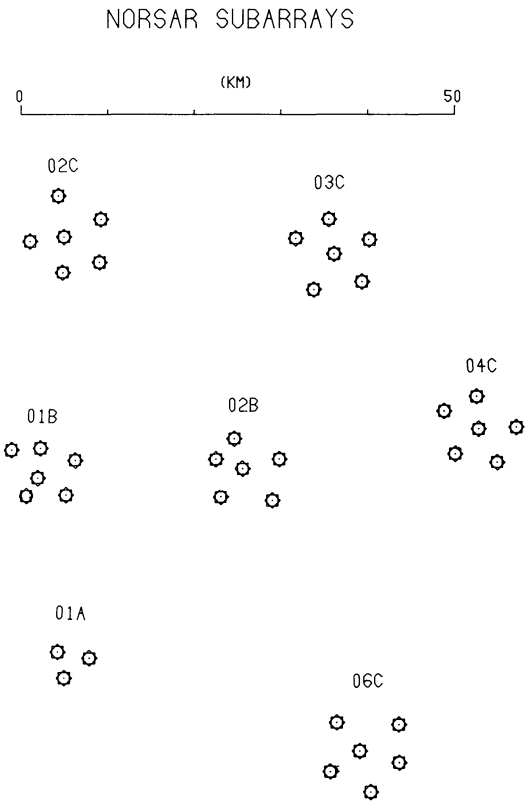

Fig. 2. The seven subarrays of the NORSAR array at the time of the FENNOLORA eyperiment. During the CAN shot, a six-element mini-array termed NORESS of diameter less than 2 km was in operation, substituting the 01B channels. NORESS is located within subarray 06C and further information is given by Mykkeltveit and Ringdal (1981)

from different azimuths swept across each of the subarrays. Because of the large number of widely spaced azimuths which were used, this experiment can be described as a large-scale fan-type one for assessing propagation characteristics from a perspective generally different from that of conventional in-line refraction profiles.

Data Analysis and Results

Record Sections

Record sections with normalized traces for each of the shot points are presented in Fig. 3a–i. The sections are arranged in order of increasing shot-point distances. The first arrivals on all the traces, hereafter referred to as *Pn*, are upper mantle waves, as the minimum recording distance was 316 km. The large, easily identifiable second arrival wave-trains seen on shots D2, E1, C1, CAN, and B3 are crustal *Pg* waves. More emergent *Pg* arrivals are seen for F1. *Pg* is observed to 700 km, and is not detected on record sections PU11, H1 and I1 (distances beyond 900 km). It must be emphasized that the symbol *Pg* as used in this paper represents the guided body wave which travels through the crust. It does not represent the refracted wave from the basement layer which is normally observed to distances up to 100 km.

Apparent Velocities and Crustal Thicknesses

Least squares apparent velocity determinations from first arrival onsets of both *Pn* and *Pg* waves are listed in Table 1. When all of the arrivals were used together, i.e., the entire distance ranges over which the phases are observed, apparent velocities of 6.36±0.02 and 8.31±0.01 km/s were found for these waves. Since there is a positive velocity gradient in the upper mantle, the *Pn* velocity just below the Moho is probably closer to 8.1 km/s, with 8.31 km/s representing an average velocity 'sampled' by rays penetrating to depths large enough to reach distances up to 1,400 km. It is interesting to note from the standard errors given that the apparent velocities for the data sets from each of the shot-points are very poorly determined and are scattered about in the 8.0–9.0 km/s range for *Pn*. Figure 4 shows a reduced travel time plot for all the arrival time data. Clearly the poor determinations of apparent velocity stem from the fact that the observational points are scattered about in clusters with little evidence of alignment within each set. This scatter of points indicates that the energy must have passed through laterally varying structures before reaching the stations.

Another very significant observation of the points of Fig. 4 is the fact that the clusters of points for *Pg* from each of the shots all tend to line up along a straight line indicating that the average nature (with the exception of thickness) of the crust sampled by the *Pg* waves does not depend on azimuth. It is well known that the *Pg* wave is a sort of guided crustal wave trapped between the surface and the large velocity gradient in the lower crust. Mereu et al. (1977) observed an à echelon pattern in the *Pg* waves

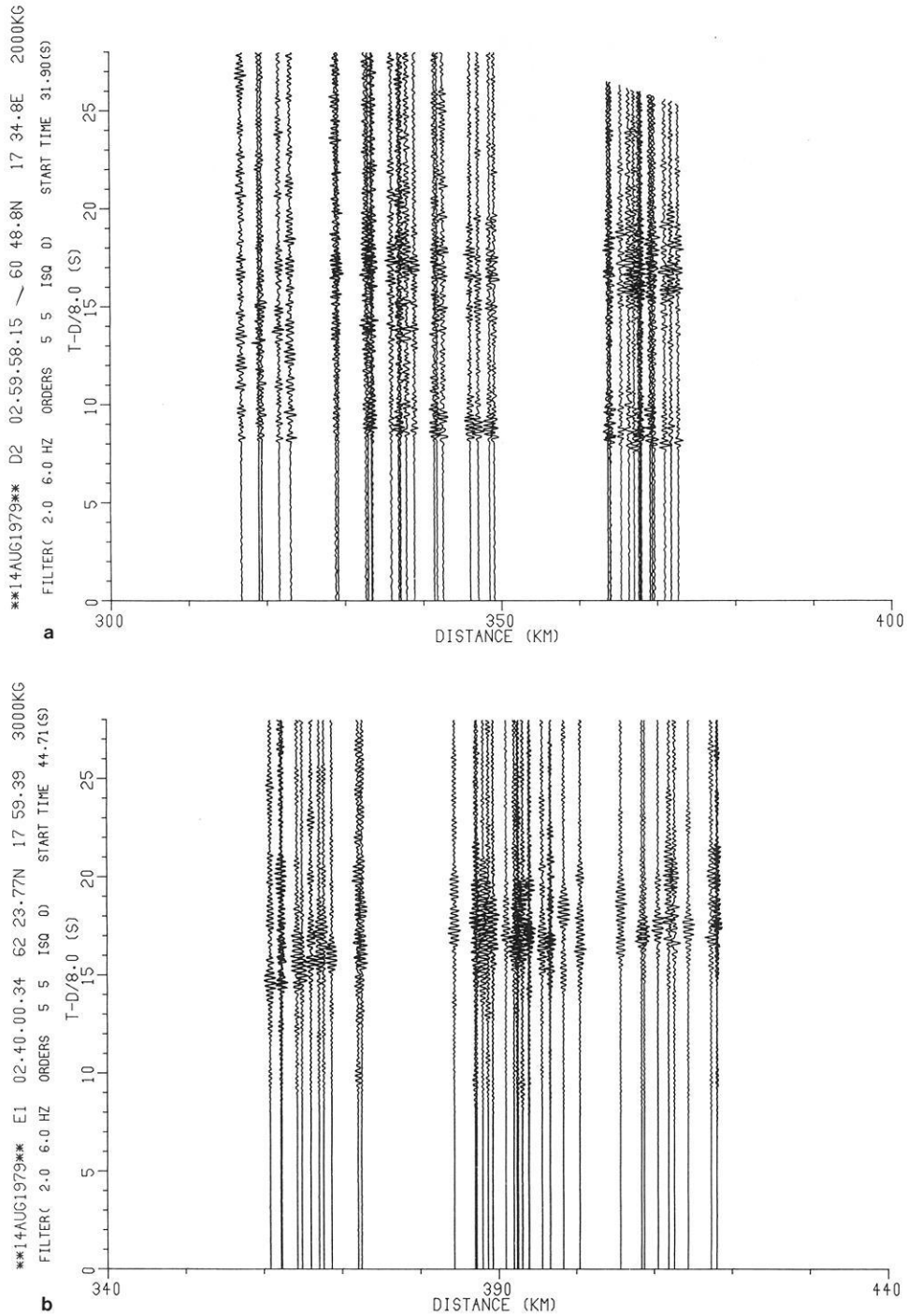

Fig. 3a–i. Seismic record sections. **a** for shot D2; **b** for shot E1; **c** for shot C1; **d** for shot CAN; **e** for shot B3; **f** for shot F1; **g** for shot PU11; **h** for shot H1; **i** for shot I1.

with short segments of these waves having relatively high apparent velocities of 6.6–6.9 km/s, while the overall apparent velocities were only 6.2 km/s. Our observations exhibit similar features. Despite the fact that the overall apparent velocity is 6.36 km/s, there are segments such as in the CAN section and in the C1 section with apparent velocities well over 6.50 km/s.

The clusters of points for the *Pn* waves are much more scattered than those of *Pg*. The reason for this is probably that the thickness of the crust, which significantly affects the travel times of the *Pn* waves, does depend on shot point locations. This is clearly seen if one compares the records of the C1 shot of Fig. 3c with the CAN shot of Fig. 3d. Both shots were at approximately the same distance from the array, but the $(Pg-Pn)$ times for the CAN shot are 2–3 s larger than the $(Pg-Pn)$ times for the C1 shot. This is a clear indication that the Moho under shot-point C is much deeper than the Moho under the CAN shot.

Further comparisons on the variation of crustal thickness with azimuth were obtained from a simple delay time analysis of the observations. The CAN shot is associated with a profile line running right into the NORSAR array (Cassell et al., in press 1983), and the thickness of the crust is found to be 28 km beneath this shot point. Now, adopt-

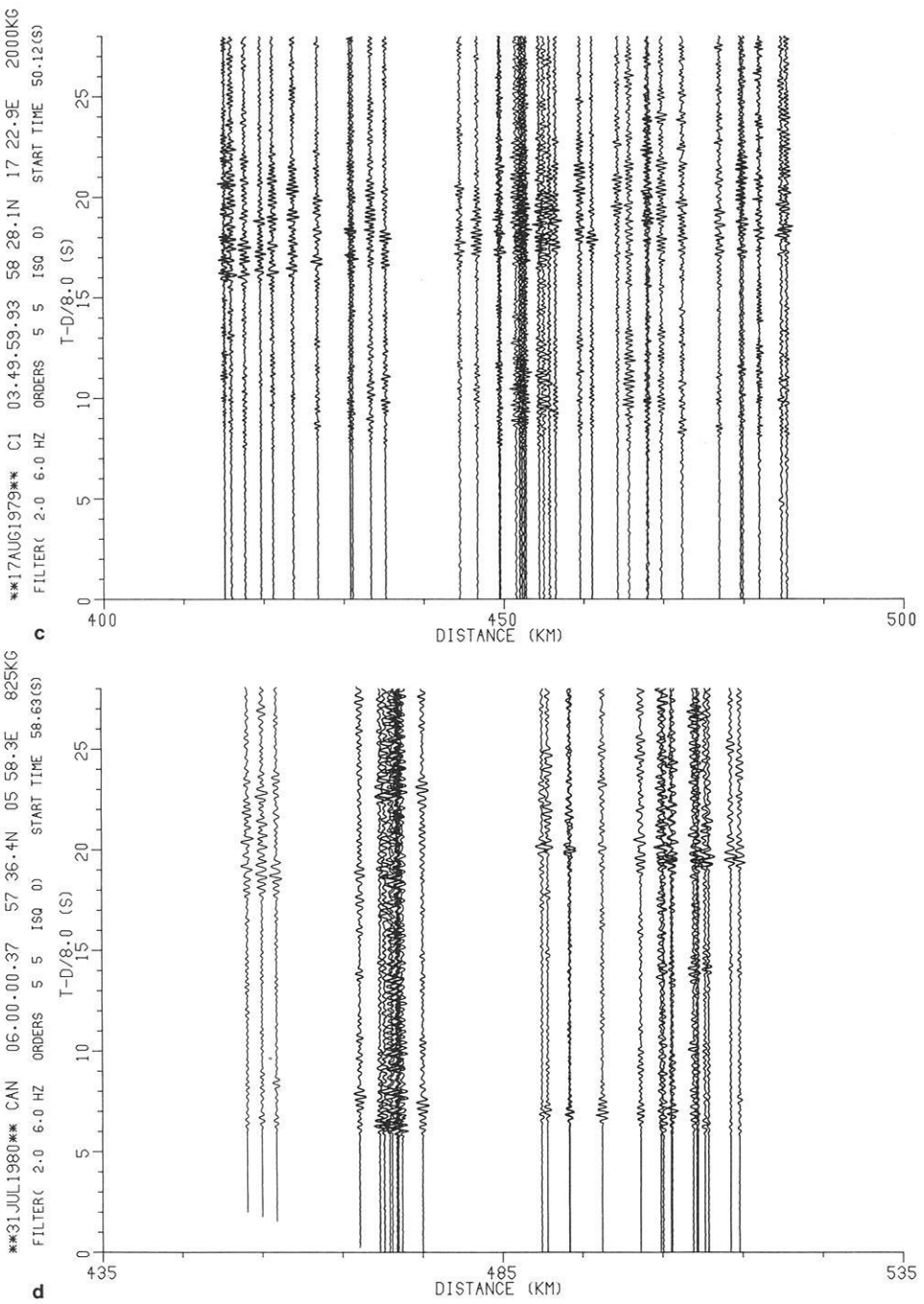

Fig. 3c–d

ing the simplified assumption that the average crustal velocity beneath all shot-points as well as average upper mantle velocity for all propagation paths (shorter than 700 km) are equal, delay time differences arise from variable Moho depths beneath the shot-points. For a fairly wide range of upper mantle velocities, a delay time difference of 1 s corresponds to a variation in Moho depth of about 10 km. 'Calibrating' against the known CAN shot Moho depth of 28 km gives crustal thicknesses of 37, 53, 51, 57 and 57 km for shot-points B, C, D, E and F, respectively. Uncertainties of these estimates are mainly tied to possible lateral variations in the *Pn* velocity. Variations in average *Pn* velocity for paths to NORSAR by as much as 0.1 km/s would contribute about 5 km to the Moho depth estimates for these shot-points.

Signal Correlation

In order to obtain the fine structure of the upper mantle it is necessary to identify and position fairly precisely later arrival branches also. A detailed analysis of the coda following the first arrival onsets was therefore undertaken using various velocity filters, envelope analysis, and correlation detectors to determine if any deterministic multiple arrivals arising from large scale regional velocity gradients were present in the upper mantle. No later arrivals, however, were found that were coherent beyond a few kilometers. The lack of coherency in most of the traces is obvious from the records in Fig. 3a–i. Some idea of the correlation distance which was observed can be seen in Fig. 5, which illustrates the normalized individual traces of the CAN shot.

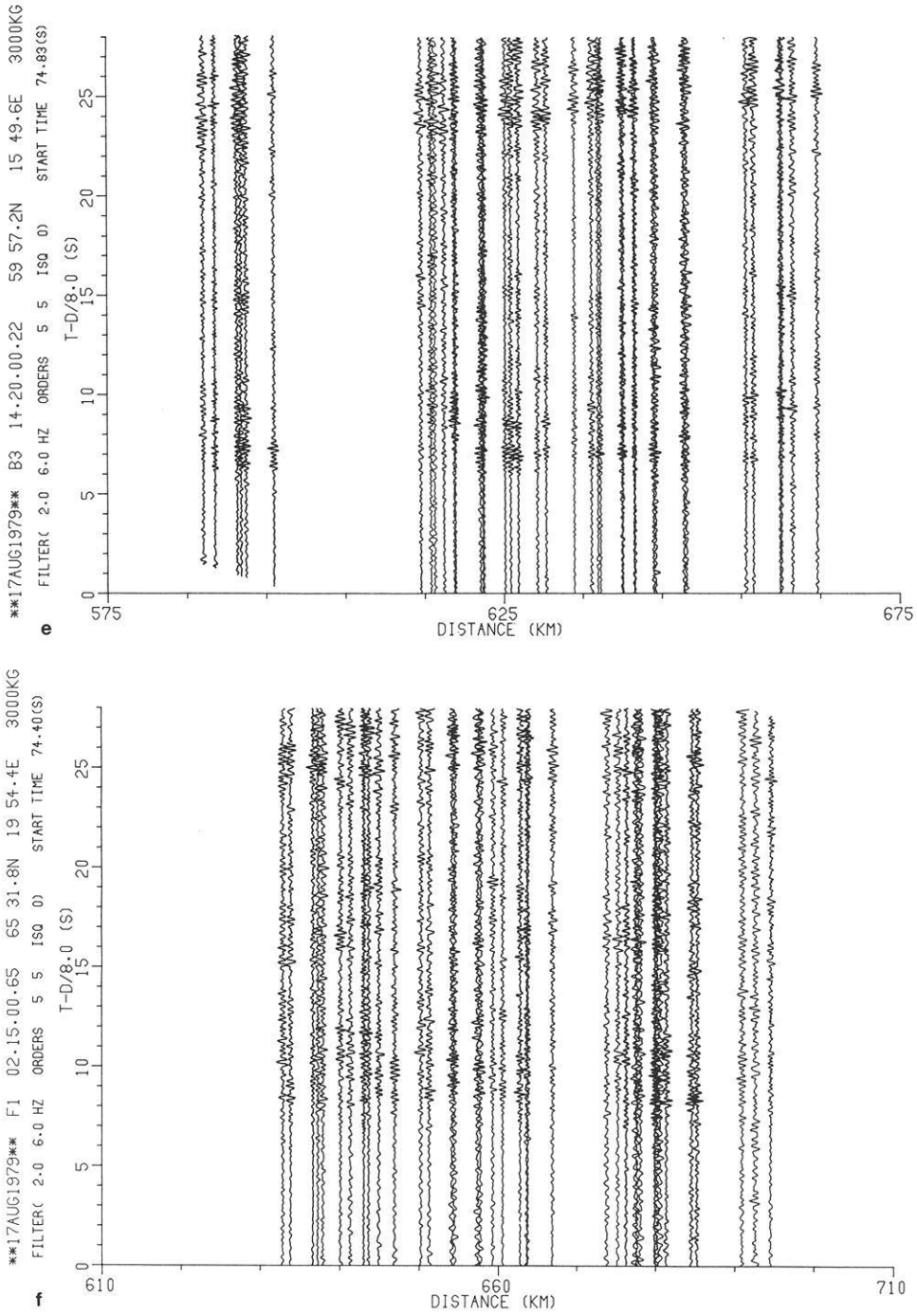

Fig. 3e–f

This figure shows that the signals correlated very well at the new NORESS subarray where the station spacing was less than 2 km, but once the distances increased beyond 2 km as was the case for the other subarrays, the correlations rapidly disappeared.

Amplitude Variations

The normalizing factors used for each trace in Fig. 5 are given under the column labelled AMP. An examination of the numbers in this column shows that large amplitude variations by as much as a factor of 5 are observed within one subarray. Compare for example trace 06C00 (AMP = 1034) with trace 06CO4 (AMP = 249). These two stations were only a few kilometers apart. Similar large scale amplitude variations were observed for the other shots. Another example is shown in Fig. 6, where the unnormalized traces of subarrays 01B and 02B for shot H1 are plotted in a record sections with an expanded distance scale. The weak amplitudes at station 01B04, the very large amplitudes at station 02B02 and the double pulse at station 02B03 all suggest that lateral structures beneath the arrays are focusing and defocusing the energy as well as creating multipath effects. Comparisons of the amplitudes observed at each subarray for different azimuths confirmed, as was expected, that the amplitude and attenuation effects were also very strongly dependent on azimuth. This dependency is illustrated in Fig. 7 which shows areal views of how the amplitudes fluctuate from station to station for two different

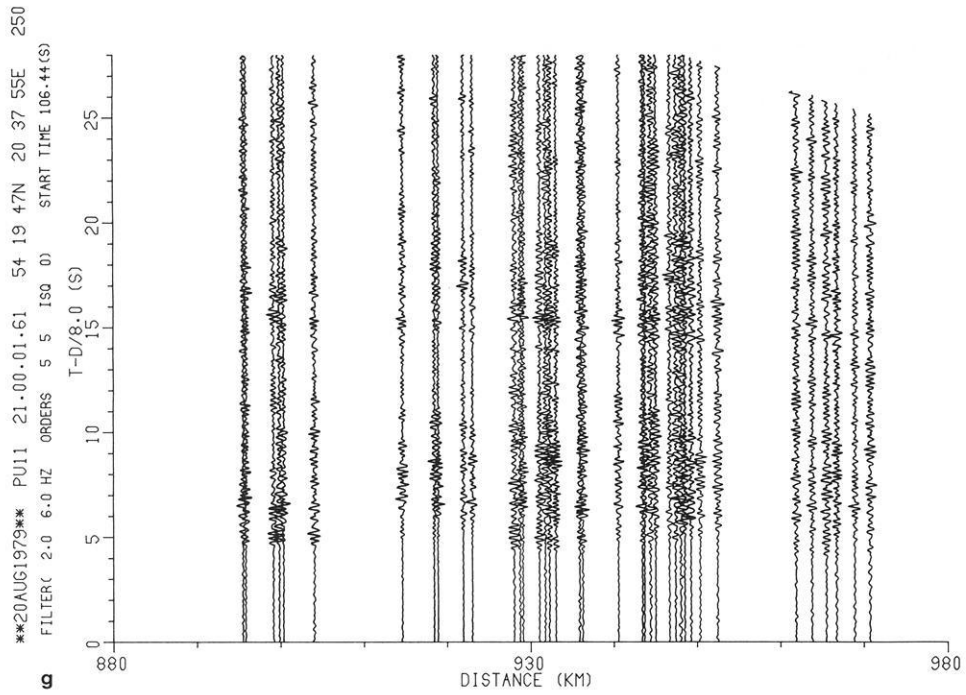

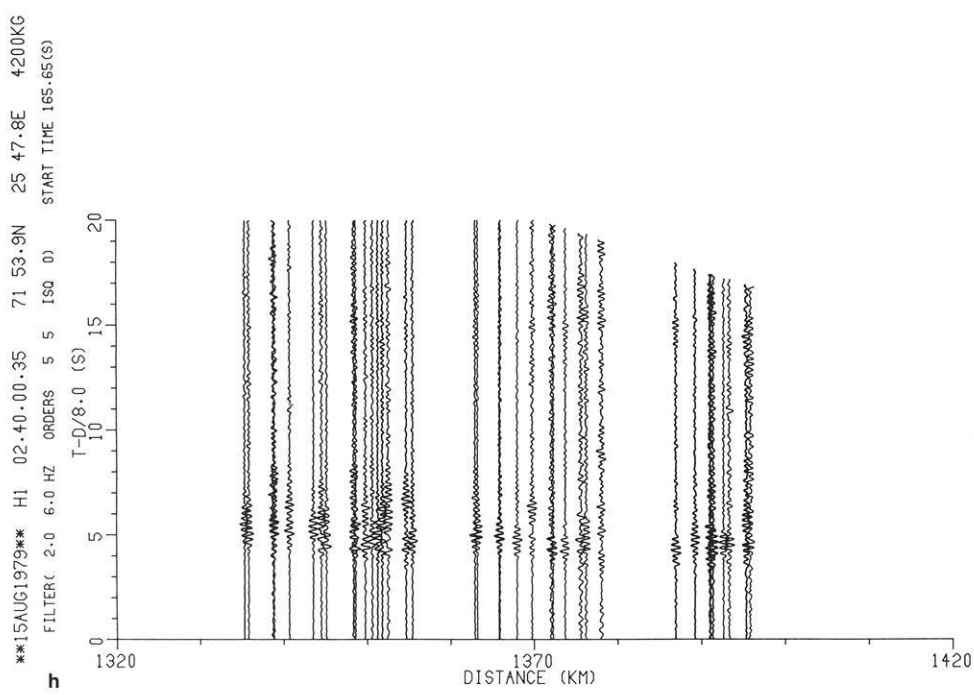

Fig. 3g–h

shots. In this figure the sizes of the various points plotted are directly proportional to the average amplitude measured over a 4 window after the onset of the arrival. The measurements were made on the envelopes of the signals. Similar amplitude fluctuations were observed for the other shots.

The amplitude data for the *Pn* waves were also compared with the corresponding data for the *Pg* waves. Figure 8 shows that rather distinct correlations exist for B3, C1 and F1, implying that local effects are amplifying and attenuating both waves together. In other cases such as CAN and E1 this relationship is lacking. The relative amplitudes of *Pn* and *Pg* for shot E1 is rather anomalous with the *Pg* amplitude being much larger than *Pn*. A comparison of Fig. 3a–c) shows that the distance range of shot E1 overlaps the ranges for shot points D2 and C1. The latter two shots have approximately the same relative amplitude for *Pg* and *Pn*. The effect is thus clearly an azimuthal effect. It should also be noted that the source function for E1 tended to have a ringing appearance which differed significantly from all the other observations. A spectrum of E1 showed a very narrow peak at 3 Hz.

Apparent Pn Dispersion

Another interesting observation may be noted in Table 1 which shows that there is a large difference in the apparent velocity of the first arrivals for H1 (8.14 km/s) from that of I1 (8.99 km/s). This seemed very puzzling at first as the

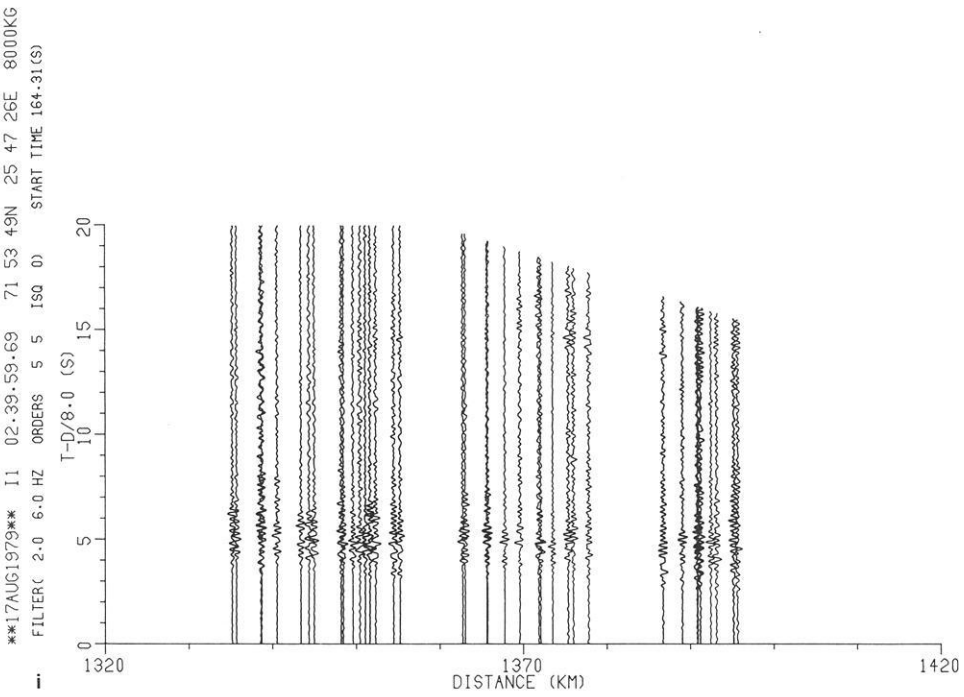

Fig. 3i

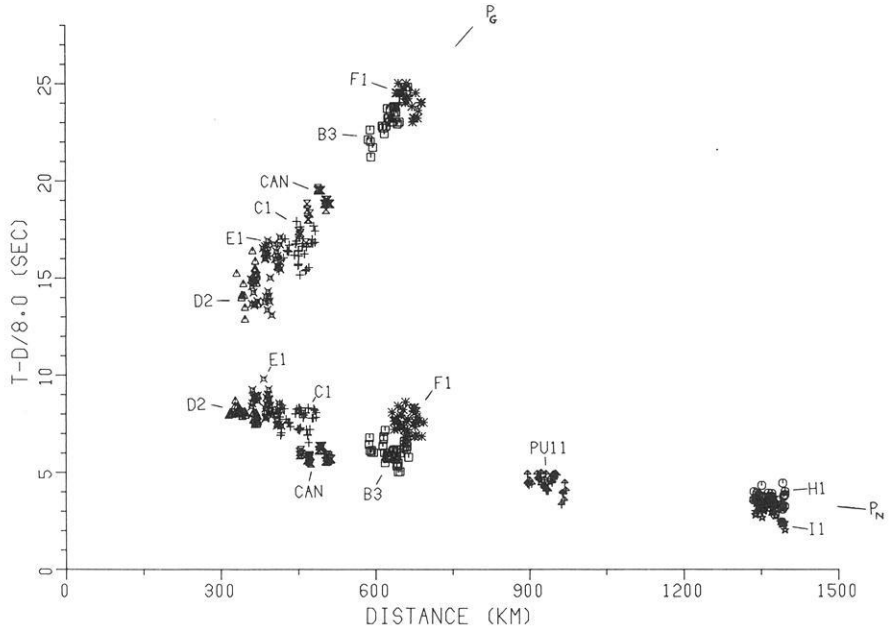

Fig. 4. Reduced travel time plot of all first onsets of crustal *Pg* waves and upper mantle *P* waves. A different symbol is used for arrivals from each shot point

two shot points were only a few hundred meters apart meaning that the travel paths were practically identical. A closer examination of this problem revealed that this effect arose because the spectrum of I1 had a much larger low frequency 2 Hz component compared to that of H1. The spectra of the 02B00 traces for these two shots are shown in Fig. 9a and b. There is no doubt that the difference in the spectral content is related to their respective charge sizes. A closer examination of the record sections showed that the higher apparent velocity for I1 came from the fact that dispersion had taken place with the lower frequency components arriving at the array about a second earlier than the high frequency components. The amplitudes of the 2 Hz waves from the H1 shot were not large enough to be detected and hence their first arrivals were later than those of I1. It thus appears that the low frequency waves have formed a shorter time path or were scattered less than the high frequency components. The dispersion referred to here is an apparent dispersion and not the true dispersion associated with anelasticity.

Beamforming and Further Processing

A search of the record sections was made using conventional beamforming and adaptive processing methods to determine if any later arrival time branches could be identified in the mantle coda. A typical example is shown in Fig. 10. This figure illustrates how beams formed from the traces

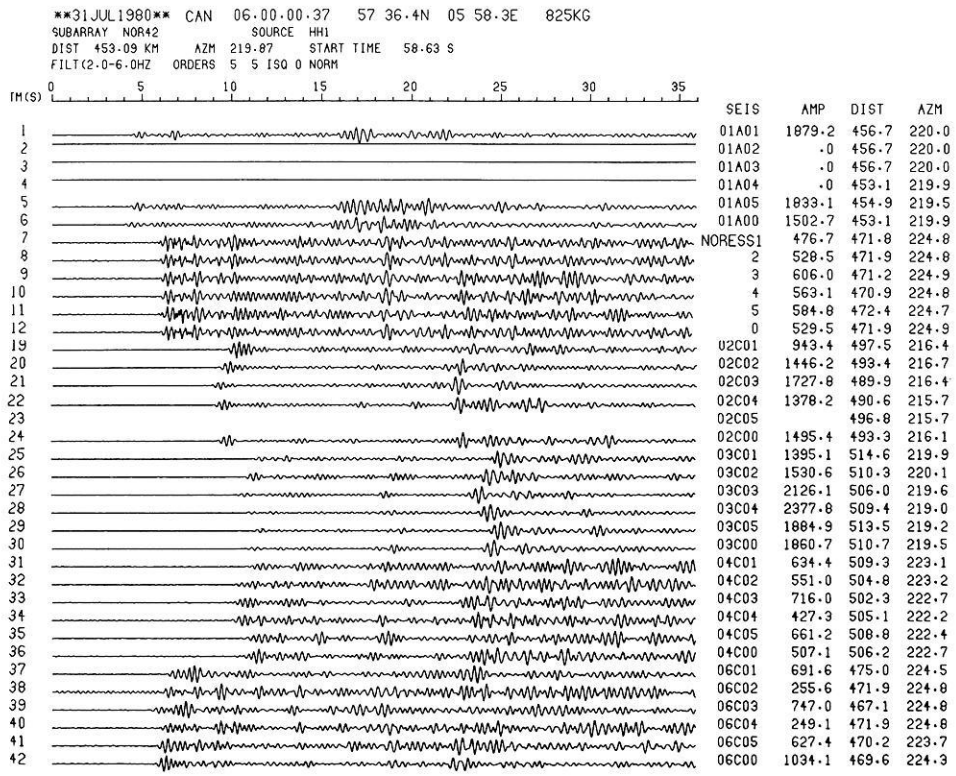

Fig. 5. Seismic traces from the CAN shot. *Note:* The coherency of the signals across the closely spaced NORESS stations and how this coherency is destroyed for the other subarrays

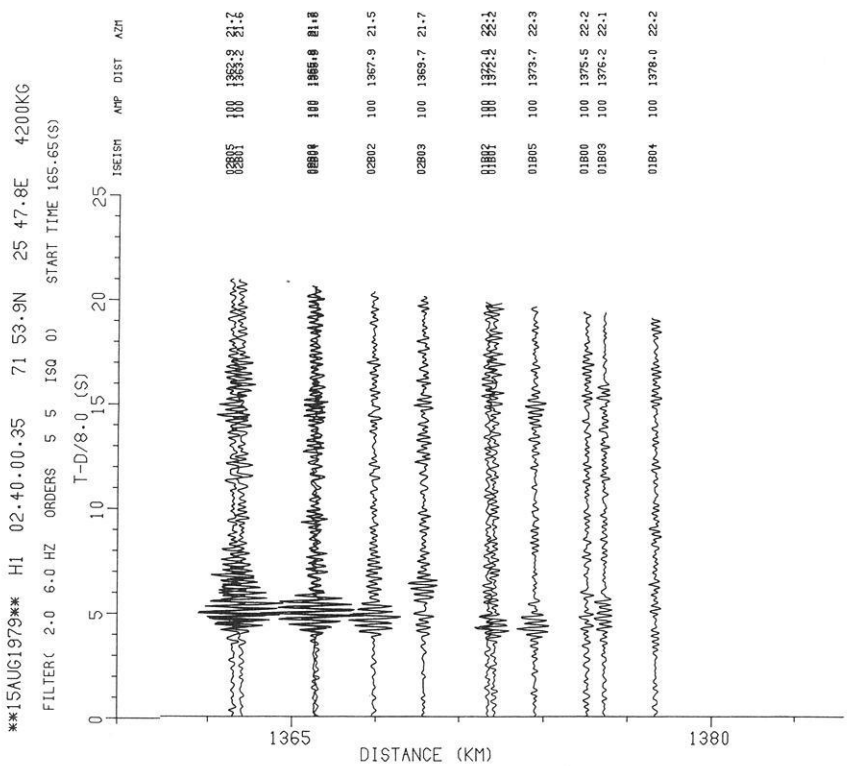

Fig. 6. Unnormalized record section for subarray 01B and 02B of the H1 shot

from 3 subarrays 1B, 2B and 2C change as beamforming velocities are varied from 7.6–9.6 km/s. No velocity creates a well-defined peak in the beam amplitudes, furthermore, because of large spatial aliasing effects in the coda noise, even the *Pg* amplitudes were not attenuated when high apparent velocities such as 9 km/s were attempted. *N*th root beamforming methods and adaptive processing methods both gave spurious results. All of these techniques are effective only for low frequency coherent signals which are characteristic of long distant teleseisms. The FENNOLORA signals have a dominant frequency of over 4 Hz and are thus much more sensitive to small-scale lateral inhomogeneities. These quickly contaminate the wavefront with the obvious effect of lost coherency.

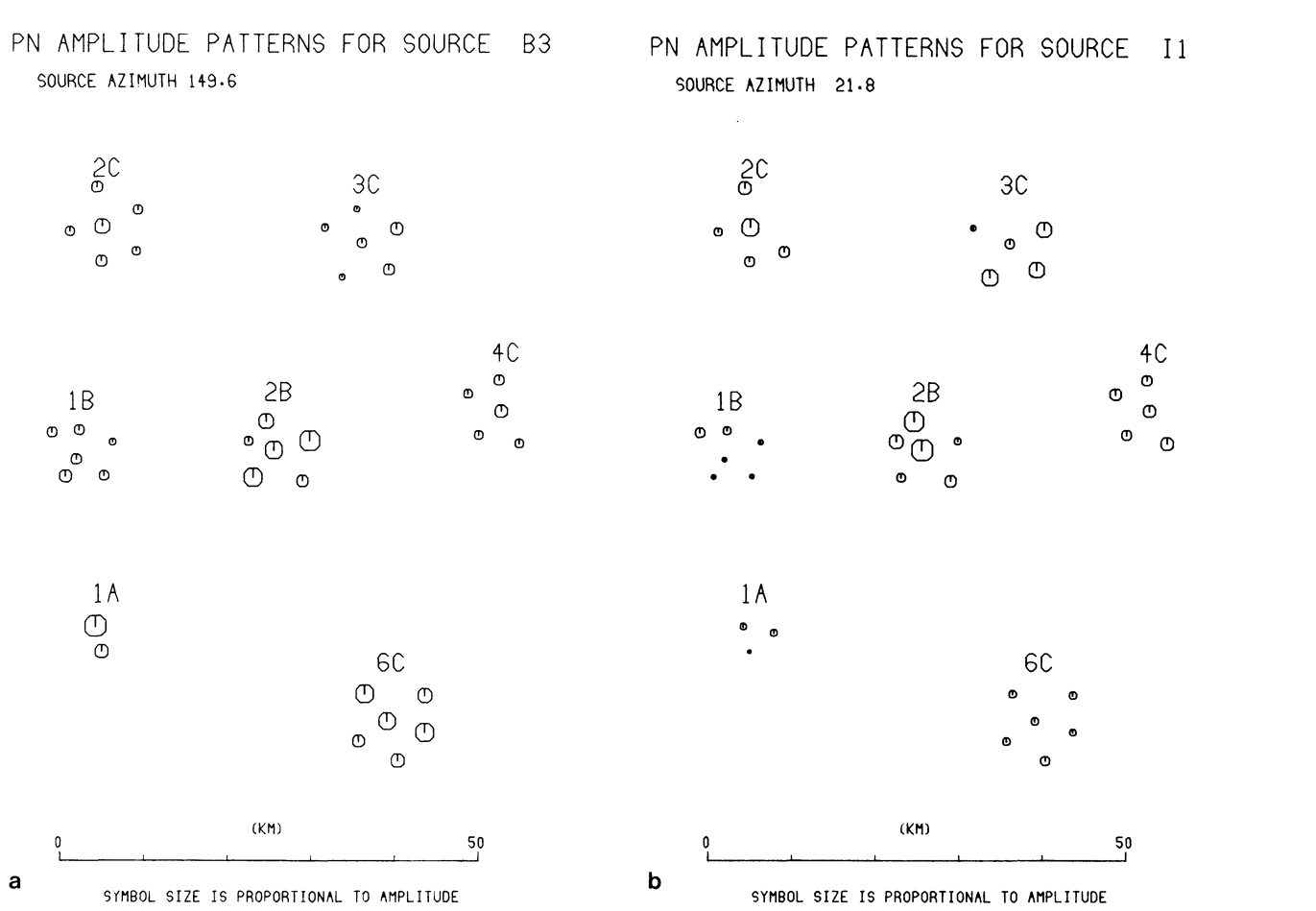

Fig. 7a and b. Observed amplitude patterns for two shots

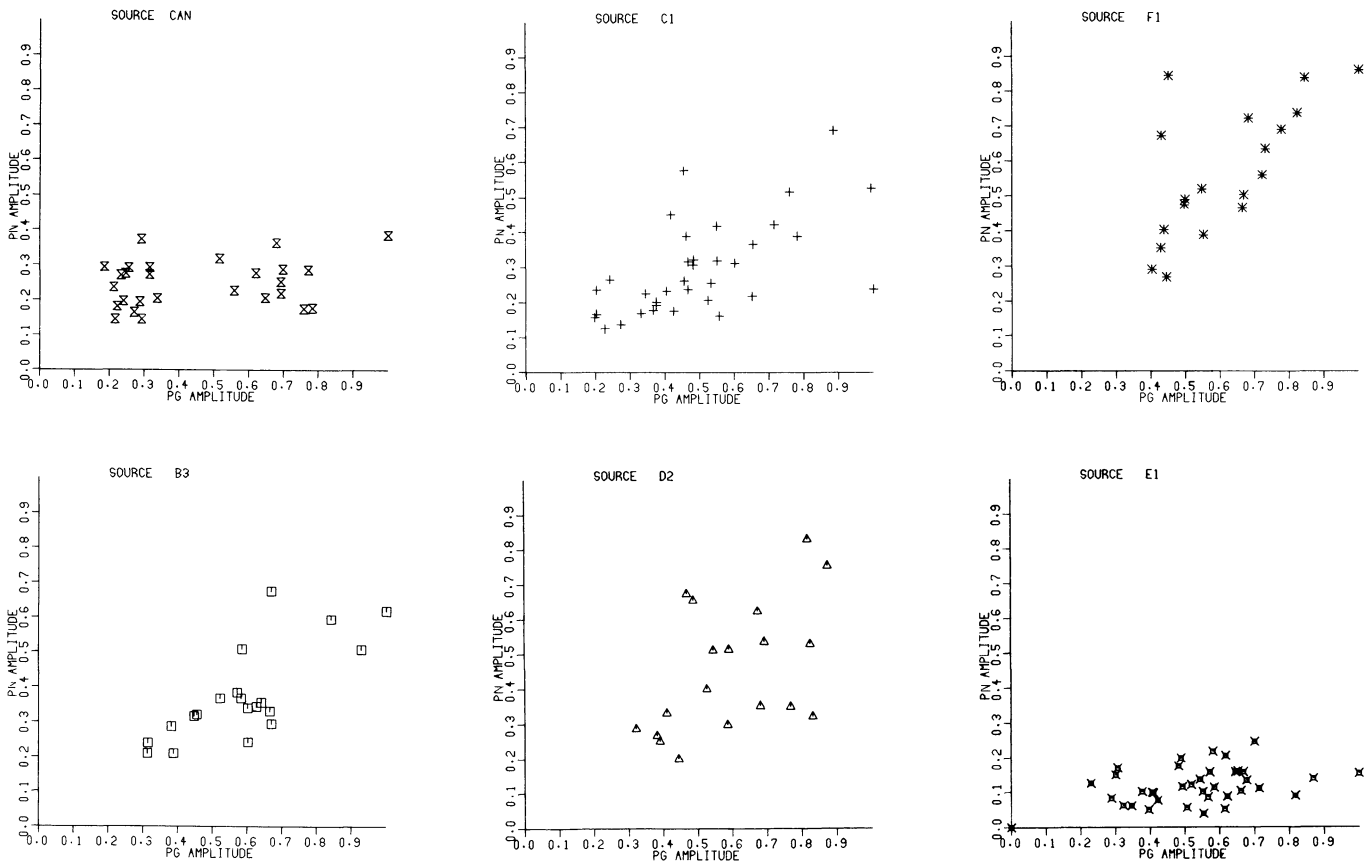

Fig. 8. Relationships between *Pg* and *Pn* amplitudes

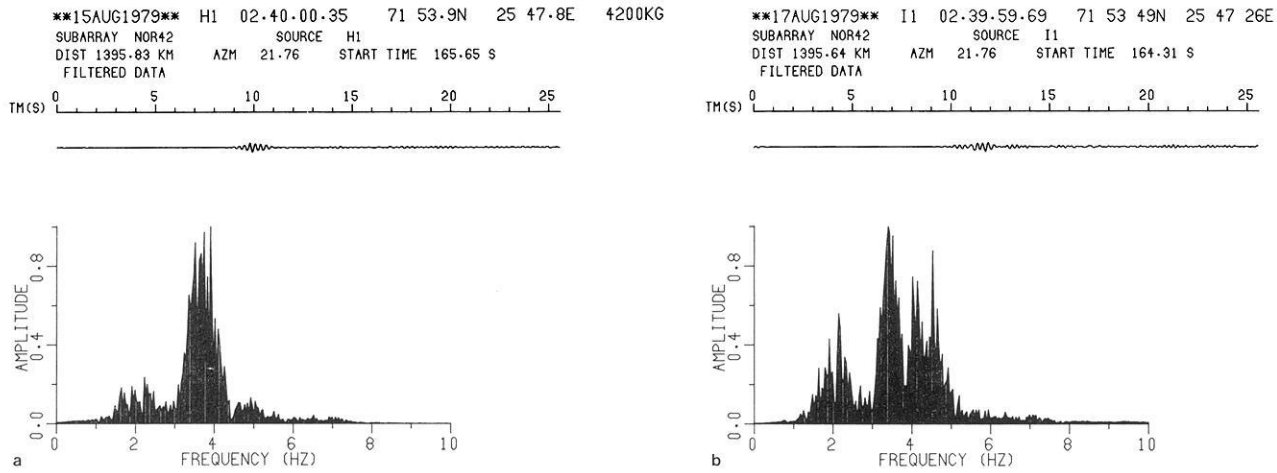

Fig. 9a and b. Signal spectra of **a** the H1 shot observed at station 02B00, **b** the I1 shot observed at station 02B00

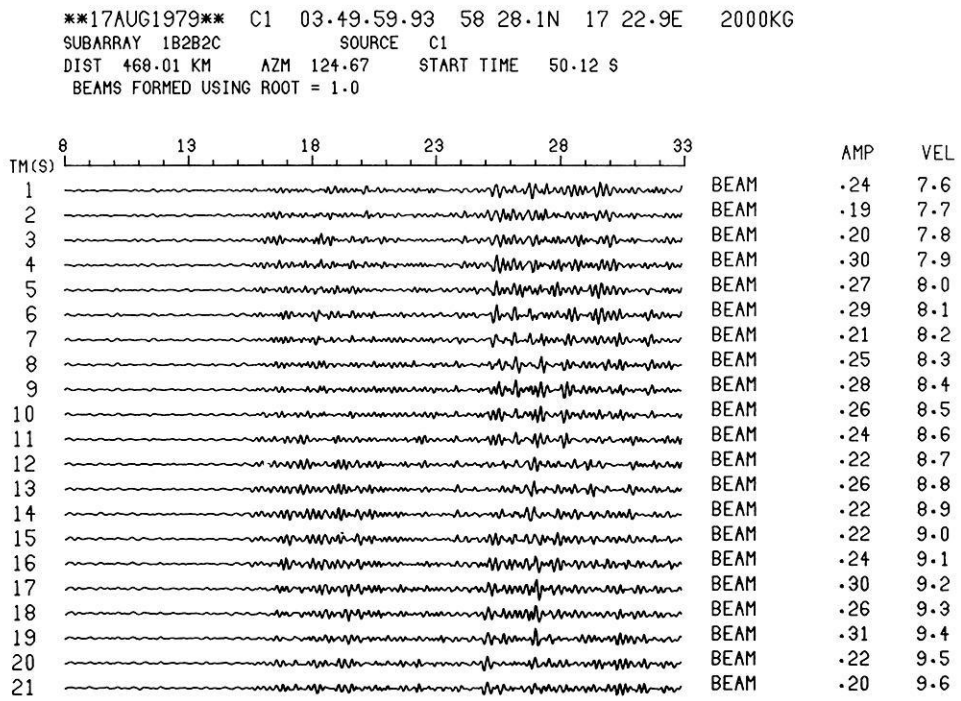

Fig. 10. Set of beams formed from traces of three subarrays (01B, 02B and 02C) for shot C1. Amp = normalizing amplitude used to normalize the traces. Vel = apparent velocity used in creating the beams

In order to get around the spatial aliasing problem and the incoherency problem, beams were also formed using envelopes of the traces. Figure 11 shows that this method is not sensitive enough to variations in apparent velocity to yield useful information.

Discussion

In long range seismic experiments numerous arrivals or energy bursts are observable in the recordings and the FENNOLORA seismograms in Fig. 3 are no exception in this respect. However, only two *P* phases can be identified with confidence, namely, the first-arriving *Pn* wave and *Pg*, the latter out to a range of 700 km. Traditionally, there has been a tendency among many controlled-source seismologists to associate secondary arrivals with multi-layered crust and upper mantle models. Others have in general been opposed to the multilayering models on the grounds of lack of objective phase identification criteria and the non-uniqueness in association of the various arrivals. The validity of these objections has been demonstrated with the now widespread use of seismogram synthesis as an analysis tool in the interpretation of refraction data. In particular, multilayered models often to not account properly for the observed amplitude distributions. We think that many features of the NORSAR FENNOLORA records and specifically the absence of clear secondary mantle arrivals can be attributed to wave scattering effects of small-scale heterogeneities particularly in the crust both at the source and receiver sides. The effect of such inhomogeneities on the amplitudes is often much more pronounced than the amplitude effects caused by possible regional discontinuities or velocity gradients. Travel time fluctuations as well as amplitude fluctuations lead to difficulties in measuring accurate apparent

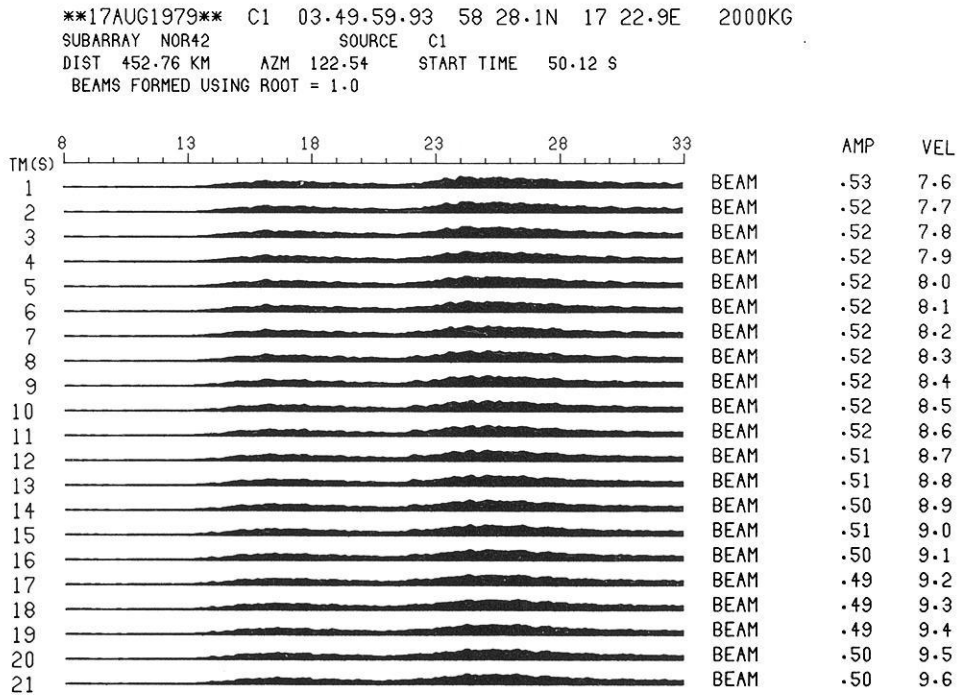

Fig. 11. Set of beams formed from the envelopes of all the traces of the NORSAR array for shot C1. Amp = normalizing amplitude used to normalize the traces. Vel = apparent velocity used in creating the beams

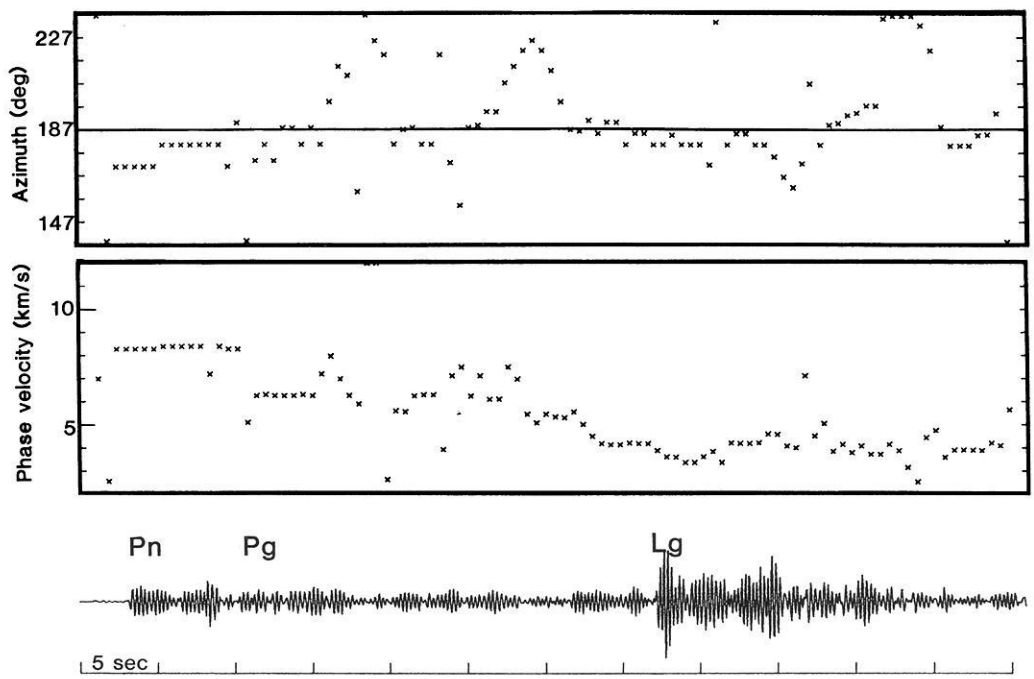

Fig. 12. Results from a sliding window frequency-wavenumber analysis of NORESS data from a presumed explosion in the sea at a distance of 260 km, direction south. At the time of this explosion NORESS had 12 sensors (data is shown for one of these) all within an area of 2 km diameter. Frequency-wavenumber analysis results in terms of phase velocity and azimuth for frequencies corresponding to the peak power are plotted for data window lengths of 2.5 s each, with time shifts of 0.6 s. The line in the azimuth diagram shows the azimuth according to the epicenter solution by the Scandinavian network of seismic stations. The uncertainty of this solution in terms of azimuth from NORESS may be as large as 5–10 degrees

velocities over a short distance even in cases where onset times are well defined. Mereu and Ojo (1981) showed, using numerical models of random media, that it is possible to have breaks in the travel time curves even though there may not be a discontinuity associated with that break. Their study showed why deep seismic reflection experiments give a different picture of the crust and upper mantle than the long-range refraction experiments.

Now, in case of the NORESS array, with sensor interspacings of the order of 125–2,000 m, even high frequency signals ($\sim$4 Hz) are coherent. We therefore took the opportunity to demonstrate in practice our comments on the im-

portance of scattering in the crust by subjecting an event, a presumed explosion in the Kattegat (Fig. 1) with features rather similar to a number of FENNOLORA recordings at NORSAR, to frequency-wavenumber analysis. The outcome of this analysis in terms of phase velocities and azimuths is shown in Fig. 12. The *Pn* wave train results imply that the various ray paths are mainly in the source-receiver plane. The *Pg* phase exhibits quite different features. This wave has been subject to strong scattering resulting in a rather weak, diffuse onset, while the relatively energetic coda appears to be made up of *Pg*-type of waves possibly reflected from the western 'wedge' of the Oslo Graben (in view of the azimuth variations). The coda of the *Lg* wave apparently also consists of significant scattering contributions.

Because of lack of correlation and presumed predominance by scattered waves we were unable as demonstrated in previous sections to utilize techniques like beamforming, envelope beamforming or adaptive processing methods for decomposing the wavetrains in phase velocity/azimuth units and thus facilitate the phase identification of even energetic arrivals. This does not preclude the existence of discontinuities in the upper mantle, but suggests that such contributions are rather insignificant in comparison to scattering arrivals. Indeed, the existence of a rather complex lithosphere beneath the NORSAR array has been repeatedly demonstrated in several studies based on a variety of approaches like random (Chernov) media modelling (Dahle et al., 1975; Berteussen et al., 1975), deterministic modelling on the basis of time and amplitude inversions (Aki et al., 1977; Christoffersson and Husebye, 1979; Haddon and Husebye, 1978) and inversion based on holographic principles (Troitskiy et al., 1981).

We have previously labelled the large difference in *Pn* phase velocities as observed from shots H1 and I1 a dispersion phenomenon. A plausible explanation is that the *Pn* path is slightly frequency dependent due to velocity gradients or heterogeneities beneath Moho. From the work of Mereu and Ojo (1981) it is not unreasonable to assume that lower frequencies which do not 'see' small-scale heterogeneities, form shorter propagation paths than higher frequencies.

Rough approximations of crustal thicknesses beneath the individual shot points can be inferred from the data at hand. Our estimate of the Moho depth beneath shot point B seems reasonable when comparison is made with previous studies (e.g., Bungum et al., 1980), while crustal thicknesses derived for C, D, E and F appear a bit excessive. In order to reduce these values to the more 'acceptable' range 41–47 km, it is necessary to infer a difference in upper mantle average velocities for paths to NORSAR by as much as 0.2 km/s between the CAN and B shots on one side and C, D, E and F on the other. Such variations are, however, larger than we would expect for the ray paths in question (Husebye and Hovland, 1982), indicating that our data point to larger Moho depths than hitherto conceived of for these areas of Sweden. We can only await the results from the FENNOLORA line for full assessment of the usefulness of NORSAR's FENNOLORA recordings in this respect.

Conclusion

Our concept of a rather simple Fennoscandian crustal/upper mantle structure is not invalidated by NORSAR's recordings of the FENNOLORA shorts. We find that short wavelength heterogeneities both at source and receiver ends contribute significantly to the observed seismogram complexities and tend to 'mask' the effects of possible large-scale regional gradients. We recommend long range profiling layouts to be supplemented with small arrays to check the extent of lateral heterogeneities.

Acknowledgements. The authors would like to thank the technical and secretarial staffs both at NORSAR and at the University of Western Ontario for their valuable assistance while conducting this research.

This research project was financed by an NTNF/NORSAR Fellowship and the Natural Sciences and Engineering Research Council of Canada (NSERC) grant no. 1793.

References

Aki, K., Christoffersson, A., Husebye, E.S.: Determination of the three-dimensional seismic structure of the lithosphere. J. Geophys. Res. **82**, 277–296, 1977

Ansorge, J.: Fennoscandia long-range project 1979 (FENNOLORA), first results, Working Group of European Seismological Commission. Presented at the 21st General Assembly of IASPEI, London, Ontario, July 1981

Berteussen, K.-A., Christoffersson, A., Husebye, E.S., Dahle, A.: Wave scattering theory in analysis of P wave anomalies at NORSAR and LASA. Geophys. J.R. Astron. Soc. **42**, 403–417, 1975

Bungum, H., Pirhonen, S.E., Husebye, E.S.: Crustal thicknesses in Fennoscandia. Geophys. J. R. Astron. Soc. **63**, 759–774, 1980

Cassell, B.R., Mykkeltveit, S., Kanestrøm, R., Husebye, E.S.: A North Sea-Southern Norway seismic crustal profile. Geophys. J. R. Astron. Soc. 72, in press 1983

Christoffersson, A., Husebye, E.S.: On 3-D inversion of P-wave time residuals: option for geological modeling. J. Geophys. Res. **84**, 6168–6176, 1979

Dahle, A., Husebye, E.S., Berteussen, K.-A., Christofferson, A.: Wave scattering effects and seismic velocity measurements. In: Exploitation of Seismograph Networks, K.G. Beauchamp, ed., Holland: Noordhoff-Leiden 1975

Haddon, R.A.W., Husebye, E.S.: Joint interpretation of P wave time and amplitude anomalies in terms of lithospheric heterogeneities. Geophys. J. R. Astron. Soc. **55**, 19–43, 1978

Husebye, E.S., Hovland, J.: On upper mantle seismic heterogeneities beneath Fennoscandia. Tectonophysics **90**, 1–17, 1982

Mereu, R.F., Majumdar, S.B., White, R.E.: Moho topography under the highest ranges of the Canadian Rockies. Can. J. Earth Sci. **14**, 196–208, 1977

Mereu, R.F., Ojo, S.B.: The scattering of seismic waves through a crust and upper mantle with lateral and vertical inhomogeneities. Phys. Earth Planet. Inter. **26**, 233–240, 1981

Mykkeltveit, S., Ringdal, F.: Phase identification and event location at regional distance using small-aperture array data. In: Identification of Sismic Sources – Earthquake or Underground Explosion, E.S. Husebye and S. Mykkeltveit, eds. Dodrecht: D. Reidel Publ. Co. 1981

Troitskiy, P., Husebye, E.S., Nikolaev, A.: Lithospheric studies based on holographic principles. Nature **294**, 618–623, 1981

Received August 27, 1982; Revised version January 31, 1983
Accepted February 1, 1983